Amperometric Electrochemical Microsystem for a Miniaturized Protein Biosensor Array

Chao Yang, Yue Huang, *Student Member, IEEE*, Brian L. Hassler, R. Mark Worden, and Andrew J. Mason, *Senior Member, IEEE*

***Abstract*—Protein-based bioelectrochemical interfaces offer great potential for rapid detection, continuous use, and miniaturized sensor arrays. This paper introduces a microsystem platform that enables multiple bioelectrochemical interfaces to be interrogated simultaneously by an onchip amperometric readout system. A post-complementary metal–oxide semiconductor (CMOS) fabrication procedure is described that permits the formation of planar electrode arrays and self assembly of biosensor interfaces on the electrodes. The onchip, 0.5-μm CMOS readout electronics include a compact potentiostat that supports a very broad range of input currents—6 pA to 10 μA—to accommodate diverse biosensor interfaces. The 2.3 $\times$ 2.2-mm chip operates from a 5-V supply at 0.6 mA. A prototype electrochemical sensor platform, including an onchip potentiostat and miniaturized biosensor array, was characterized by using cyclic voltammetry. The linear relationship between the oxidization peak values and the concentrations of target analytes in the solution verifies functionality of the system and demonstrates the potential for future implementations of this platform in high sensitivity, low cost, and onchip protein-based sensor arrays.**

***Index Terms*—Amperometric readout, bioelectronic sensor, biosensor array, complementary metal–oxide semiconductor (CMOS) potentiostat, electrochemical sensor.**

I. Introduction

MEASURING analyte concentrations is essential for a wide range of applications, including the study of biological systems, quality control, high-throughput drug screening, disease diagnosis and treatment, and biological threat detection. Electrochemical biosensors have been widely used to determine the analyte concentrations, both in research and commercial applications [1]–[4]. A broad range of protein classes can be employed as the biological recognition elements (BRE) in electrochemical biosensors that measure analyte concentrations directly, or indirectly, through electrochemical reaction coupling [5]–[9]. Electrochemical sensors typically utilize three-electrode electrochemical measurement techniques and interface with electronics through a potentiostat, which can be configured for potentiometric or amperometric operation. Electrochemical biosensors offer advantages over optical measurement techniques [10]–[12], including the elimination of performance-limiting optical interference and the ability to directly perform electrical signal processing without extensive external equipment. Furthermore, the miniaturization potential of electrochemical biosensor arrays [13] makes the cost-effective, chip-scale integration of the entire analysis platform possible.

Miniaturization of biosensor elements increases their sensitivity and permits the integration of sensor arrays with a large number of detection sites and diverse functionalities, enabling massively parallel biorecognition capability. Miniaturization also makes the system more cost-effective because it utilizes batch fabrication manufacturing processes and requires only small volumes of potentially expensive reagents. Biosensors based on soluble and membrane proteins that are tethered to planar electrodes [14]–[16] have the potential to be durable and reusable and are ideally suited to build low-cost miniaturized arrays for many applications. Working toward a microsystem that integrates a miniaturized protein biosensor array with the required measurement electronics would fuse the advantages of miniaturization with improved measurement accuracy due to the elimination or reduction of external noise sources. Furthermore, the compact size and built-in intelligence of an integrated microsystem platform would simplify measurement setup and enable widespread usage in laboratories or field environments. However, there are challenges in the miniaturization and integration of protein-based biosensors and their instrumentation electronics that remain to be addressed. Microsystems that integrate DNA sensor arrays [17] and single redox analyte sensors [18] have been reported. However, these platforms are not suitable for the amperometric readout of protein-based biosensors due to incompatibilities in structure/fabrication and the absence of the necessary signal extraction techniques. Recently, a microsystem that integrates an amperometric potentiostat circuit and an onchip electroactive polymer film array was developed [19], but its sensitivity and dynamic range are not appropriate for protein-based biosensors.

To physically link protein biosensors with their instrumentation electronics, a post-complementary metal–oxide semiconductor (CMOS) fabrication procedure tailored to this platform is needed. The fabrication procedure must provide an

Manuscript received May 14, 2008; revised October 23, 2008. First published April 28, 2009; current version published May 22, 2009. This work was supported in part by the Engineering Research Centers Program of the National Science Foundation (NSF) under Award Number EEC-9986866, NSF Award Number DBI-0649847, in part by the Michigan Economic Development Corporation's MTTC program, and in part by the MSU Foundation's Strategic Partnership Grant program. The paper was recommended by Associate Editor Pedram Mohseni.

C. Yang is with Marvell Semiconductor, Inc., Santa Clara, CA 95054 USA (e-mail: yangchao@marvell.com).

Y. Huang, B. L. Hassler, R. M. Worden, and A. J. Mason are with Michigan State University, East Lansing, MI 48824 USA (e-mail: huangyu3@msu.edu; hasslerb@msu.edu; worden@egr.msu.edu; mason@msu.edu).

Color versions of one or more of the figures in this paper are available online at http://ieeexplore.ieee.org

Digital Object Identifier 10.1109/TBCAS.2009.2015650

array of electrode transducers while maintaining compatibility with CMOS electronics and self-assembled biosensor interfaces. To exploit the sensitivity of miniaturized protein-based electrochemical BREs [14], the readout electronics must be highly sensitive and noise resistant. To support diverse classes of proteins, the instrumentation circuits must accommodate a wide range of signal strengths, ∼120 dB based on reported miniature biosensors. For amperometric detection, these requirements translate to current sensitivities ranging from 10 pA to 10 μA. Several integrated-circuit (IC) amperometric readout circuits have been previously reported, including high resolution circuits using charge integrators that convert currents to voltages or digital pulses [17], [20]–[26]. While the reported sensitivities are sufficient for this application, new instrumentation circuits are needed that provide a very wide input current range and all of the necessary bias and stimulus control to accommodate protein-based electrochemical biosensor interfaces.

In this paper, a new miniaturized electrochemical biosensor platform with onchip potentiostat and biosensor readout circuitry is introduced. In Section II, the system architecture for rapid detection, continuous use, and biosensor array is developed. In Section III, a CMOS-compatible (post-CMOS) fabrication procedure for electrode transducers, self-assembled biointerfaces, and fluid handling are described. The design of the onchip instrumentation circuitry that supports a wide range of on or offchip sensor elements and several interrogation techniques is discussed in Section IV. In Section V, test results for the circuit and a prototype sensor array are presented, demonstrating the feasibility of this microsystem platform.

II. System Architecture and Requirements

In constructing a system for protein-based electrochemical biosensor arrays, the composition of the system is determined almost entirely by the physical and electrical requirements associated with forming the biointerfaces and continuously monitoring their activity. Several protein classes, which can be roughly grouped into soluble and membrane proteins, are good candidates for miniaturized electrochemical sensors. A key challenge in biosensor development is assembling interfaces that simultaneously immobilize the protein on the electrode in an active conformation and allow the protein's activity to be measured. A common approach is to use conductive or electroactive molecular components to chemically tether the protein to planar gold electrodes [2], [27]. Acting as the physical and electrical interface between the biological and electronic components, the electrodes are required to maintain compatibility with both components. Therefore, to support a fully onchip integrated microsystem platform, the electrode material and fabrication process are required to be post-CMOS compatible (i.e., able to be performed after CMOS circuit fabrication without affecting circuit performance).

A variety of electrochemical methods can be utilized to monitor protein activity, including voltammetry and impedance spectroscopy. Initially, our paper has focused on several voltammetry techniques, requiring a transducer system composed of a reference electrode (RE), a counter electrode (CE), and an array of working electrodes (WE). To complete the electrochemical measurement system, the instrumentation electronics must incorporate an amperometric readout and the electrode bias and control necessary for voltammetry techniques. All of the required instrumentation circuitry should be integrated into a single microelectronics chip to support system miniaturization and the related cost, performance, and application advantages. To maintain versatility in the microsystem platform, the electrodes and instrumentation chip must permit either a hybrid (multiple components) or monolithic implementation. From the electrode point of view, this means developing a flexible fabrication process that allows a range of electrode sizes and geometries, thus supporting the needs of different biointerfaces and applications. From the instrumentation point of view, this means that a large range of amperometric inputs must be supported.

For reduction-oxidation reactions, the current I generated by the sensor can be estimated by

$$I = AnF\Gamma T \tag{1}$$

where A is the electrode area, n is the number of electrons involved in the reaction, F is Faraday's constant, Γ is the surface coverage density of the protein, and T is the turnover rate [19]. For our previously reported 90-μm electrodes [28], the response current was about 10 pA for a secondary alcohol dehydrogenase (2° ADH) modified electrode, based on reported turnover rates (from 100 s^{-1} to 1000 s^{-1}) and surface coverage (10^{-11} mol cm^{-2}) [2]. Alternatively, to support centimeter sized offchip electrodes, the maximum current could reach 10 μA. Thus, the readout circuit must support a very wide input current range—from 10 pA to 10 μA. In practice, the electrode area can be very precisely defined, with good repeatability, using photolithography. However, it is typically difficult to precisely control the density of protein on each electrode and, thus, calibration would be needed for individual electrodes.

The microsystem architecture shown in Fig. 1 was developed to handle all of the requirements described before. Composed of a silicon chip with CMOS instrumentation circuits and an enzyme functionalized electrode array, this microsystem represents the long-term vision guiding the developments presented in this paper. For high throughput applications, solutions can be delivered from the top by a robotic fluid delivery system and extracted by external pumps. The electrochemical readout chip can be wire bonded to the package substrate to receive configuration commands and transmit measurement data. Alternatively, the electrode array can be offchip, where the resulting hybrid microsystem achieves the same functionality but trades reduced packaging complexity for the performance gain of monolithic integration.

III. Biosensor and Electrode Array Fabrication

We have developed a variety of protein interfaces compatible with the requirements from Section II and the microsystem concept shown in Fig. 1. Designed for self assembly on planar electrodes, these interfaces, and several others currently under development, can be tethered to electrode arrays, providing the biological recognition elements of the electrochemical microsystem.

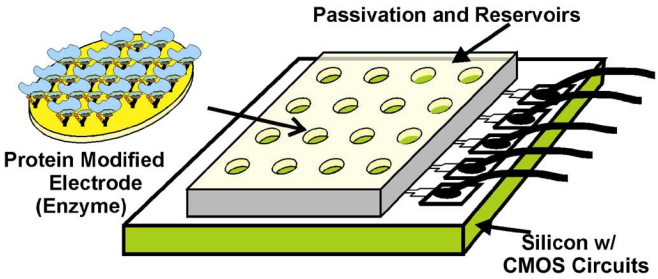

Fig. 1. Conceptual architecture of an electrochemical protein biosensor array microsystem.

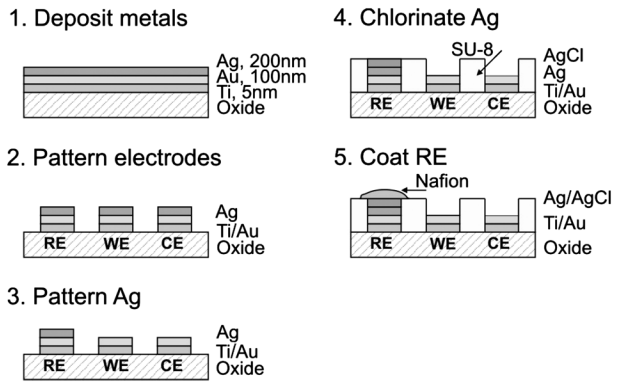

Fig. 2. Electrochemical electrode array-fabrication procedure.

Using photolithography-based techniques, we have developed a procedure for fabricating electrode arrays and fluid handling structures that are suitable for either monolithic or hybrid configurations [14], [29]. By altering mask patterns, the size and geometry of the electrodes can be easily varied, and a number of different electrode arrays have been fabricated. For a typical array, Fig. 2 shows that the electrodes are constructed by depositing a 5-nm titanium (Ti) adhesion layer under a 100-nm gold (Au) layer and patterning the layers by using photolithography. Gold was chosen because it is biocompatible, is relatively inert, has a relatively wide electrochemical potential window, and permits immobilization of the biointerfaces through the strong thiol-Au coupling. Since the surface will be exposed to a liquid environment, a passivation layer (typically crosslinked SU-8 photoresist) is deposited over the electrodes and patterned to form reservoirs that contain solutions during biointerface self assembly. The passivation layer overlaps the edge of the working electrodes to prevent corrosion of the Ti layer and current leakage through the Ti layer at the edge of the electrodes. To maximize continuity of the biointerface along its edge, the passivation layer is patterned to form circular working electrodes, although Ti/Au traces beneath the passivation layer can be in any shape.

Requiring only low-temperature thin-film deposition and photolithography, the electrode formation process is suitable for post-CMOS fabrication. Fig. 3 illustrates a typical structure resulting from this process, and it shows how the surface Ti/Au electrodes can be routed to CMOS metals through openings in the overglass layer. Since the surface of a CMOS chip has a dielectric coating, the electrode fabrication procedure is equally suitable for making offchip arrays on glass substrates.

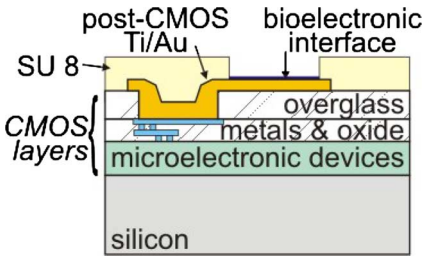

Fig. 3. Cross-sectional view of an onchip Ti/Au electrode.

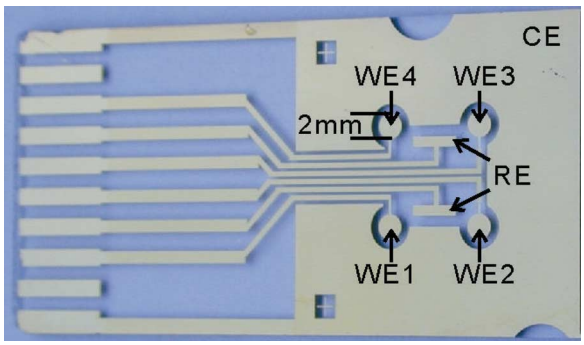

Fig. 4. Photograph of an offchip Ti/Au electrode array on glass.

Fig. 3 shows one of these devices with a 2 × 2 array of working electrodes (WE1-4), a large-area counter electrode, and two quasireference electrodes. Such offchip arrays simplify packaging and handling issues and permit the use of larger electrodes that do not require robotic fluid delivery equipment for interface assembly. Therefore, to permit rapid prototyping of the sensor array system and characterization of the amperometric readout chip, the offchip array shown in Fig. 4 was used to obtain the results described in this paper. This permits us to address several challenges toward a fully integrated microsystem, as outlined in the Introduction, and demonstrates a platform that is useful to alternative applications where less expensive, disposable sensor components are desirable.

IV. Potentiostat VLSI Realization

An interface circuit is needed to drive the three electrodes of an electrochemical sensor array system and provide an amperometric readout for the array's current response. To support diverse high sensitivity biosensors, the circuit must accommodate a wide range of input currents and feature low noise. The principal schematic of the interface circuit designed to achieve these goals is shown in Fig. 5. The function of each block was explained in Section II, and the VLSI realization of these blocks will be described.

A. Potentiostat Structure

In the electrode potential drive block of Fig. 5, control signal $Vsrc$ sets the potential applied across the electrochemical cell, and either a constant voltage or a sweeping signal, for cyclic voltammetry (CV) can be applied. $Amp2$ is configured as a unity gain buffer to sense the RE potential without loading the RE. The WE is connected to the negative input of the leftmost OTA through the MUX, and WE's potential was set to the OTA's positive input (system reference potential) by the feedback loop

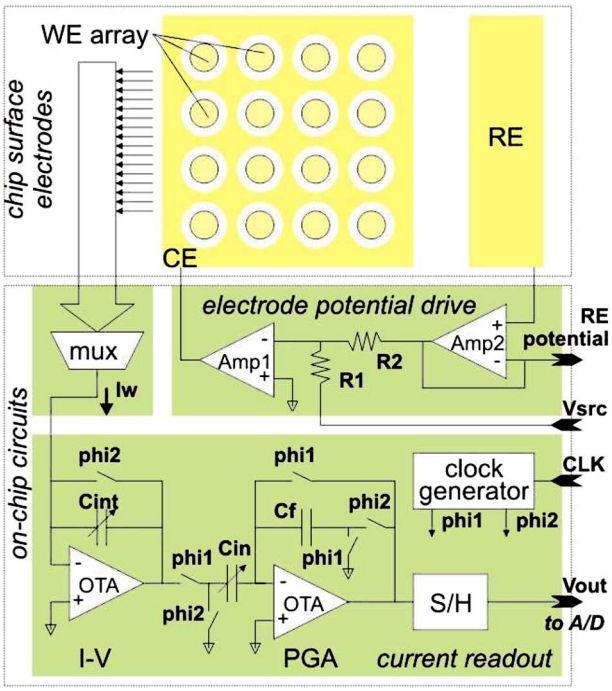

Fig. 5. Schematic of the surface electrode array and the onchip potentiostat comprised of a switched capacitor amperometric readout block, an electrode potential drive block, and a current switching matrix (mux).

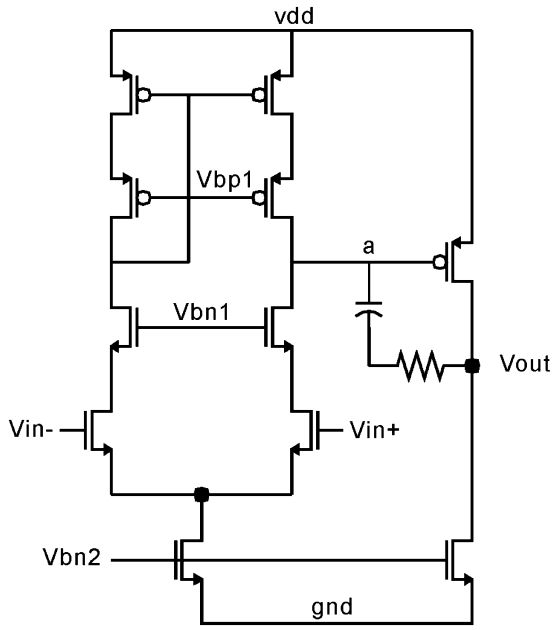

Fig. 6. Schematic of the two-stage amplifier.

formed with Cint. With the link formed by the electrolyte solution between CE and RE, $Amp1$ and $Amp2$ form a feedback circuit to establish a potential difference between the RE and the chosen WE, which is at the system reference potential. Notice that the RE cannot sink/source electrical current, so all current measured at the WE comes from the CE, which helps maintain stability of the RE electrochemical potential.

In the current readout block [28], a switched-capacitor (SC) charge integrator converts the biosensor current response into voltage, which then goes through a programmable gain amplifier (PGA). The output of the PGA is sampled, held, and fed to an analog-to-digital converter (ADC). The entire readout chain utilizes the correlated double sampling (CDS) technique [30] to reduce the $1/f$ noise as well as amplifier offset. The output of the current readout block $V_{\rm out}$ is given by [31]

$$V_{\rm out} = \frac{I_w}{C_{\rm int} f_s} \cdot \frac{C_{\rm in}}{C_f} \tag{2}$$

where f_s is the frequency of $phi1$, I_w is the sensor current from the working electrode, $C_{\rm int}$ is the integrator capacitor, $C_{\rm in}$ is the binary weighted programmable capacitor at the PGA input, and C_f is the feedback capacitor of the PGA.

The sensitivity of biointerfaces attached to a WE can vary widely, resulting in a broad range of response currents. Variability in the WE area for different arrays extends the response current range even more. Thus, the current readout block was designed to operate over a wide range of input currents. As shown in (2), the readout circuit gain $(V_{\rm out}/I_w)$ is determined by the clock frequency, the PGA gain $(C_{\rm in}/C_f)$, and the value of the integrator capacitor. Thus, by using onchip-programmable capacitors for $C_{\rm int}$ and $C_{\rm in}$ and adjusting the clock frequency, the readout circuit can be adapted to a large span of input currents. The capacitor values and operational frequency were selected to support a very broad range of currents—from 10 pA to 10 μA.

To achieve high sensitivity in the current readout circuit, care was taken to minimize the noise power of the amplifiers. Also, the CDS technique was employed to sample and subtract a portion of the $1/f$ noise and clock feedthrough charge, thereby suppressing noise at the output. Minimum-sized complementary CMOS switches were used to minimize charge injection.

B. Amplifier Topology

Two amplifiers were designed for the readout circuit to support different loading characteristics. The amplifiers used in the potentiostat drive block must drive the biosensors, which have complicated impedance characteristics. In order to maintain the system stability with variable loading, a two-stage amplifier was designed so that the dominant pole is located inside the amplifier and is independent of the loading conditions. Alternatively, the amplifiers in the current readout block have purely capacitive loading of a known value. Thus, cascode single-stage amplifiers were employed to reduce hardware by eliminating the Miller compensation components. With the dominant pole located at the output node, purely capacitive loading only improves the phase margin.

A schematic of the two-stage amplifier is shown in Fig. 6. With Miller compensation, the internal (dominant) pole at node a and the output pole are split away from each other. Simulation shows that this amplifier has 110-dB dc gain and at least 3.5-MHz unit gain bandwidth with expected variations in loading conditions. For bioelectrochemical applications, the frequency of the stimulus is always very low (i.e., less than 100 Hz). The dc gain and the bandwidth are large enough to ensure

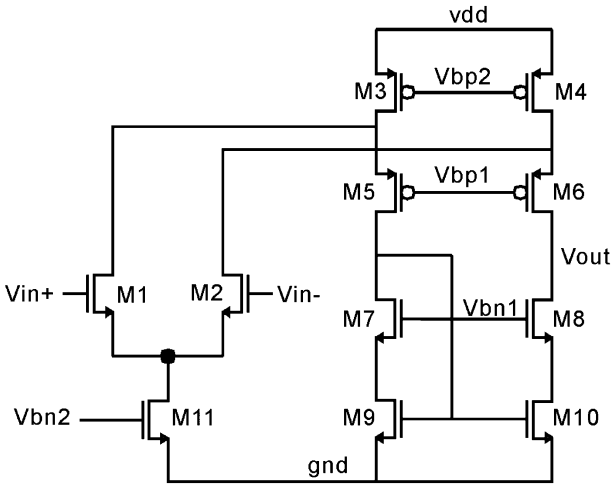

Fig. 7. Schematic of the folded cascode OTA.

that the electrode potential drive stage can transfer the stimulus to the sensors accurately.

An operational transconductance amplifier (OTA) configuration was chosen for the switched-capacitor (SC) current readout block. The two main design considerations for this OTA are: 1) high gain, to ensure precision operation and 2) rapid settling time to ensure that the output settles within half the clock period. Fig. 6 shows the schematic of the OTA that meets these requirements. The single-stage configuration of the OTA enables wide bandwidth, and the folded cascode structure provides high dc gain and wide dynamic range. The simulated performance of this circuit shows a dc gain of 79 dB, a unity gain bandwidth of 24 MHz, with a 60° phase margin, 49 $\mathrm{V}-\mu\mathrm{s}^{-1}$ slew rate, 33-ns settling time, an input/output range of 0.8 V to 3 V, a CMRR of 107 dB (dc), and a PSRR of 80 dB.

C. Noise Analysis and Low-Noise Design

The noise performance for the electrode potential drive block is not critical because the stimulus signal for amperometric interrogation is normally several hundred millivolts, well above the noise level. However, in the current readout block, noise performance will significantly affect readout sensitivity because the response current of the biosensor could be very small (in sub-pA range). Thus, care was taken to minimize the noise power of the amplifiers in the current readout block. Although subthreshold operation generally affords better noise performance, the amplifiers were designed to operate above threshold to provide wide bandwidth and support a sampling clock rate up to 2 MHz with good accuracy. Noise analysis for these amplifiers shows that only devices in the signal path are important, and noise in the cascode devices and M11 can be ignored. The resulting input referred noise spectrum of the readout amplifier can be expressed as

$$\frac{\overline{v_{n,in}^2}(f)}{\Delta f}=2\left[\overline{v_{n1}^2}(f)+\left(\frac{g_{m3}}{g_{m1}}\right)^2\overline{v_{n3}^2}(f)+\left(\frac{g_{m9}}{g_{m1}}\right)^2\overline{v_{n9}^2}(f)\right] \tag{3}$$

where $\overline{v_{ni}^2}(f)$ represents the noise spectrum for the ith transistor due to both thermal and $1/f$ component and g_{mi} is the transconductance of transistor Mi. Substituting the thermal and $1/f$ noise models [32] of M1, M3, and M9 into the input voltage yields

$$\begin{aligned}\frac{\overline{\mathrm{v_{n,in}^2}(\mathrm{f})}}{\Delta \mathrm{f}}=&\frac{16\mathrm{kT}}{3\sqrt{2\mu_\mathrm{n}\mathrm{C_{ox}}(\mathrm{W/L})_1\mathrm{I_{DS1}}}}\\&\times\left(1+\sqrt{\frac{2\mu_\mathrm{p}(\mathrm{W/L})_3}{\mu_\mathrm{n}(\mathrm{W/L})_1}}+\sqrt{\frac{(\mathrm{W/L})_9}{(\mathrm{W/L})_1}}\right)\\&+\frac{2\mathrm{k_{fn}}}{\mathrm{C_{ox}(WL)}_1}\frac{\Delta \mathrm{f}}{\mathrm{f}}\\&\times\left[1+\frac{2\mu_\mathrm{p}\mathrm{k_{fp}}}{\mu_\mathrm{n}\mathrm{k_{fn}}}\left(\frac{\mathrm{L}_1}{\mathrm{L}_9}\right)^2+\left(\frac{\mathrm{L}_1}{\mathrm{L}_3}\right)^2\right].\end{aligned} \tag{4}$$

This equation shows that increasing W/L for the input devices and increasing the tail current will decrease the thermal noise. Since $\mu\mathrm{n} > \mu\mathrm{p}$, an amplifier with NMOS transistor inputs has less thermal noise than one with the PMOS transistor input devices. Since the SC configuration will suppress $1/f$ noise, the input devices were chosen to be NMOS with their size optimized to 150 μm/1.8 μm. With the correlated double sampling (CDS) technique, $1/f$ noise and the clock feedthrough charge can be sampled and subtracted and are therefore suppressed at the output stage. All switches were realized with complementary transmission gates of minimum size to minimize the charge injection, and dummy switches were used to reduce clock feedthrough errors.

Since the frequency range of the stimulus is always less than 100 Hz, a bandwidth of 100 Hz was chosen to evaluate the noise performance. Simulation shows an input referred noise current of 100 $\mathrm{fA/Hz^{1/2}}$ around 100 Hz and an integrated noise current power in a 100-Hz bandwidth of less than 1 pA; thus, the circuit permits a sub-pA input current resolution.

V. Testing and Results

A. Chip Implementation

The amperometric readout circuit was fabricated in a 0.5 μm CMOS process. Fig. 8 shows the 2.3 × 2.2-mm die with circuit blocks labeled. This version of the chip facilitates a 4 × 4 array of 100-$\mu\mathrm{m}^2$ working electrodes, although the circuit and post-CMOS process can be scaled to much higher density, covering the entire surface of the chip. With existing techniques and equipment, the array density is ultimately limited by fluid handling constraints to approximately ten electrodes per mm^2 chip area.

B. Potentiostat Transfer Function Characterization

To test circuit performance during cyclic voltammetry operation, a fixed-value discrete test resistor was biased by the electrode potential drive block to create a current source. This current source was then measured by the current readout block to record the potentiostat transfer function. The test resistor was placed between the WE and RE/CE nodes, with the RE and CE electrode shorted together in the absence of an electrolyte solution.

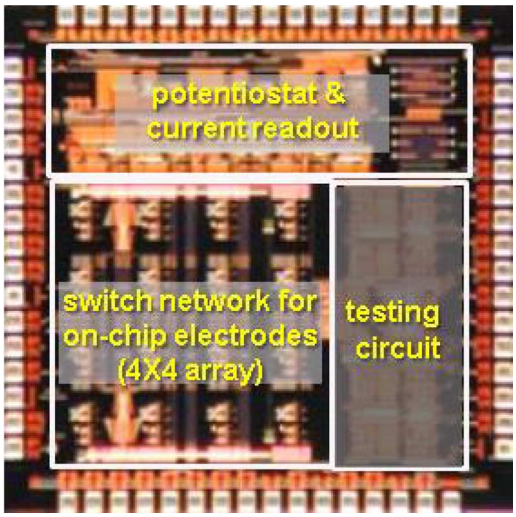

Fig. 8. Die photograph of the 2.3 × 2.2-mm CMOS chip with the onchip switch network to multiplex among 4 × 4 top metal contacts, which can connect the post-CMOS gold electrode through the overglass openings.

To measure readout sensitivity in the lowest current range, a 10-MΩ test resistor was used, and a dc sweep of the bias potential at the $Vsrc$ node (Fig. 5) was performed so that the stimulus on the resistor was ±10 mV, corresponding to a current source in the ±1-nA range. The current readout results of this dc sweep, sampled at 200 Hz, are plotted in Fig. 9(a) along with the error from the linear regression line (normalized to the 1-nA full output range). The secondary vertical axis in Fig. 9(a) shows that the measurement error is less than 0.6% of 1 nA, which corresponds to a sensitivity of 6 pA (0.6% of 1 nA). The observed error reflects the random noise in the resistor test source and the readout circuit. Leakage constraints prevent further improving the sensitivity by lowering the sampling clock below 100 Hz.

To measure the input signal in the high current range, a test resistor of 10 kΩ was used in a similar manner as before, with the sampling clock set to 2 MHz. The measured output voltage and normalized error from the linear regression line are plotted in Fig. 9(b). With a stimulus sweep of ±100 mV, the corresponding current response range is ±10 μA. A 2-MHz sampling clock reaches the bandwidth limitation of the readout channel; a higher frequency clock will result in signal distortion.

For both plots in Fig. 9, the small normalized error from the linear regression line demonstrates the good linearity (less than 0.6% normalized error) of the potentiostat over its extremely wide input current range: 6 pA to 10 μA. The whole circuits consume less than 600 μA with a 5-V supply for all of the applicable updating clock frequencies. The performance of the onchip potentiostat is summarized in Table I.

C. Platform Experiment With Biosensors

To characterize chip performance within an actual bioelectrochemical sensor system, a prototype sensor array was constructed by using electrode microfabrication procedures described before and an interface for secondary alcohol dehydrogenase (2° ADH) enzyme. Dehydrogenase enzymes catalyze a wide variety of reactions involving medically important metabolic intermediates and, thus, biosensors that either

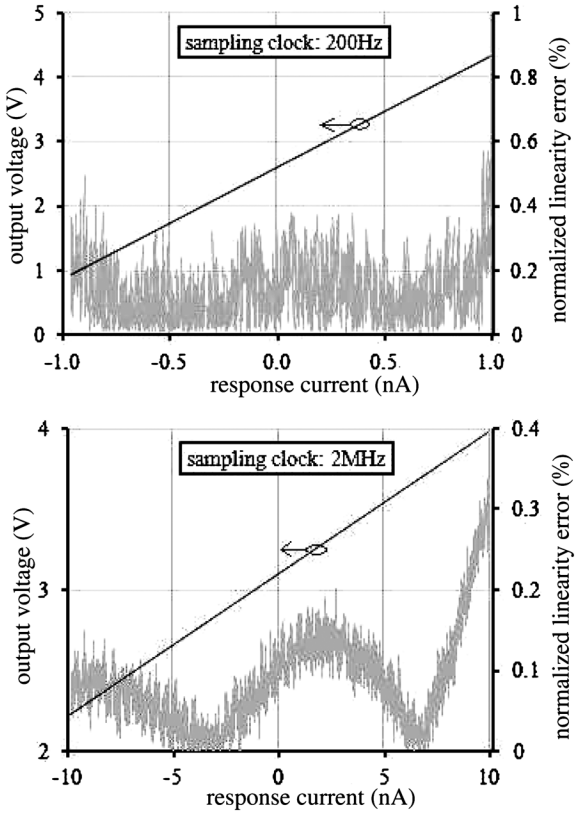

Fig. 9. DC sweep measurements of the potentiostat with a pure resistor. The output voltage and the full range normalized error from the linear regression are plotted against the input current level. The horizontal axis is the responding current of the resistor. (a) The resistor value of 10 MΩ had a stimulus swing of +/−10 mV and an updating clock of 200 Hz. (b) The resistor value is 10 kΩ with a stimulus swing of +/−100 mV and an updating clock of 2 MHz. These plots show that this potentiostat can accommodate wide input current range with good linearity (less than 0.6% error).

TABLE I
ONCHIP POTENTIOSTAT PERFORMANCE SUMMARY

Parameters	Performance
Technology	AMI 0.6μm CMOS
Chip Area	2.3x2.2mm
Power supply	5V
Power consumption	0.6mA
Sensitivity	6pA
Measurement range	10uA

use dehydrogenases to measure the concentrations of intermediates, or measure the effect of inhibitors on dehydrogenase activity have many biomedical applications [33], [34]. Since many dehydrogenase enzymes share a common cofactor, the biosensor interface represents a platform to work with a variety of dehydrogenase enzymes. In this study, 2° ADH was selected as the model dehydrogenase to demonstrate the performance of the electrochemical microsystem. This highly stable enzyme has been well characterized in a variety of bioelectronic interfaces [2], [14], [35] and is representative of interfaces that would result from dehydrogenases with biomedical relevance.

The test setup for the resulting electrochemical biosensor prototype system is described in Fig. 10. The readout chip testing

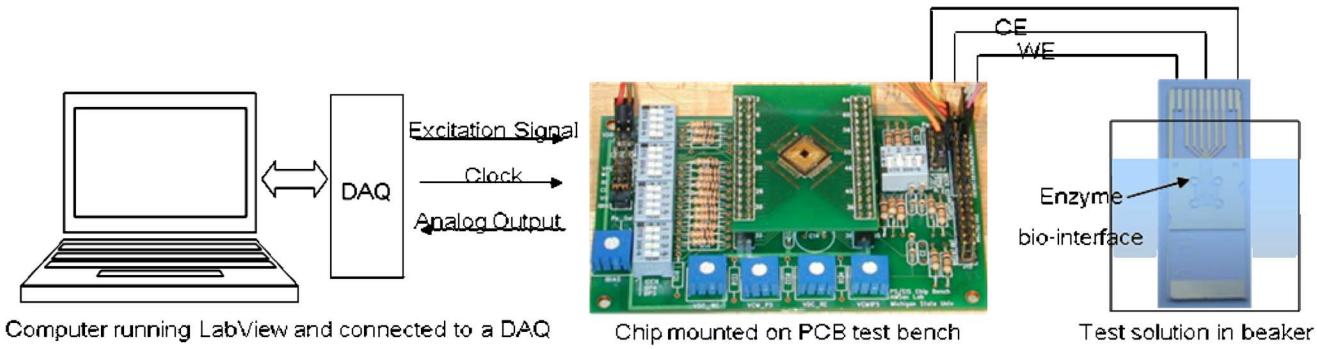

Fig. 10. Testing setup for the biosensor microarray-based onchip platform.

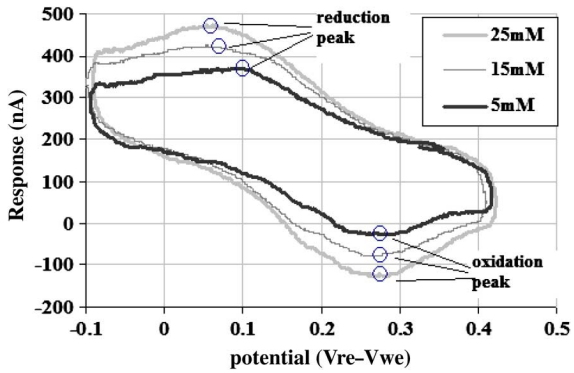

Fig. 11. Cyclic voltammograms of the $\mathrm{MPA-TBO-PEI-NADP^{+}-2^{\circ}}$ ADH functionalized electrode in the presence of different concentrations of 2-propanol: (1) 5, (2) 15, and (3) 25 mM. The data were recorded in room-temperature PBS at a potential scan rate of 100 mV s.

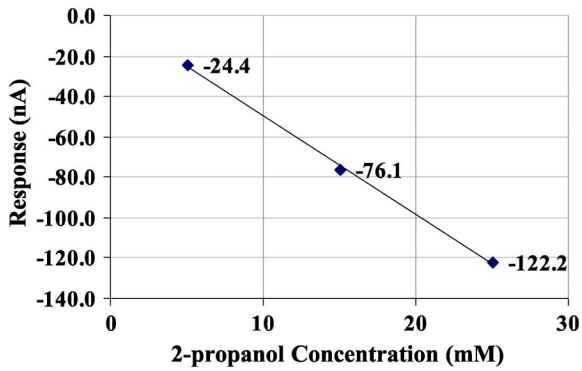

Fig. 12. Measured peak electrocatalytic current at various 2-propanol concentrations demonstrating the good linearity of the sensing system as evidenced by a high $\mathrm{R^2}$ value (0.9989).

printed-circuit board (PCB) was constructed to link the chip to the sensor array and to a computer through a National Instruments NI USB-6259 data-acquisition (DAQ) system. A LabVIEW (Austin, TX) was used to generate the desired sweeping pattern by controlling the dc supply, system reference potential, master clock signal, and potentiostat control voltage delivered to the chip. The user interface also records the chip's amperometric readout output and the actual potential at the RE, and it plots the readout circuit's output versus electrochemical cell potential to produce a cyclic voltammogram while the control voltage is swept at variable speeds. Cyclic voltammetry experiments were chosen to demonstrate the functionality of the potentiostat for this powerful technique commonly used to analyze the performance of amperometric biosensor interfaces. The height of the resulting oxidation and/or reduction peaks provides quantitative information about substrate concentration.

Each WE on the prototype array measured 1 mm in diameter and was modified using 3-mercaptopropionic acid (MPA), toluidine blue O (TBO), β-nicotinamide adenine dinucleotide phosphate $(\mathrm{NADP^{+}})$ and 2° ADH, as previously described [2]. For the readout circuit, the supply voltage was set to 5 V. A 530 mV peak-to-peak triangle wave was generated between the CE and a chosen WE, sweeping from -100 mV to 430 mV with respect to an RE absolute potential of 1.715 V, relative to the chip's ground. The onchip amperometric readout circuit was clocked at 100 kHz, and the current response of the sensor was extracted from the potentiostat circuit's voltage output.

Fig. 11 shows the cyclic voltammograms of the $\mathrm{MPA-TBO-NADP^{+}-2^{\circ}}$ ADH-modified electrode at varying 2-propanol concentrations in a 0.1-M phosphate buffer solution (PBS). Characterization versus the selected 2-propanol concentrations permits direct comparison to published performance of the 2° ADH interface. All measurements were performed at room temperature $(25 \pm 2^{\circ}\mathrm{C})$ at a scan rate of 100 $\mathrm{mV\ s^{-1}}$ with a Ag/AgCl reference electrode. As expected, the measured peak oxidation current increased linearly $(\mathrm{R^2} = 0.998)$ with 2-propanol concentration, as shown in Fig. 12. The slope of the calibration curve is a measure of the biosensor's sensitivity; the sensitivity obtained using the onchip potentiostat, 0.62 $\mu\mathrm{A\ mM^{-1}\ cm^{-2}}$, is on par with the value measured for the same interface by using commercial benchtop instruments $(2.5\ \mu\mathrm{A\ mM^{-1}\ cm^{-2}})$ [35].

These experiments verify that each critical element within the proposed biosensor microsystem platform functions as desired. The electrode microfabrication process yields a high quality link between the electrode and biosensor interfaces. The onchip potentiostat and amperometric readout circuit accurately measure the biosensor response and successfully perform cyclic voltammetry with a wide range of variable measurement parameters to suit many different sensor interfaces. These results justify continued research to fully integrate the circuit and sensor components onto a single-chip platform in order to further improve performance, reliability, and manufacturability.

VI. Conclusion

This paper introduced an electrochemical microsystem for protein-based biosensor arrays. The system is composed of protein interfaces, microfabricated electrodes, and an IC electrochemical instrument. The system architecture meets the requirements for rapid response, continuous use, and high density biosensor arrays. The biosensor interfaces were engineered to be tethered to planar electrodes and allow the measurement of enzymatic activity through electrochemical interrogation. An electrode fabrication process was outlined that satisfies the constraints in forming a biointerface array on the surface of a CMOS chip. Based on photolithography, the process permits electrode size and geometry to be readily adjusted to meet diverse application needs. The electrode microfabrication process was utilized to construct offchip arrays on glass substrates. A new versatile electrochemical instrumentation chip that provides electrode bias control and amperometric readout was described. The chip was fabricated in 0.5-μm CMOS and supports a variety of voltammetry techniques, including cyclic voltammetry and chronoamperometry. Measurements show that the chip can perform amperometric readout over a very wide input signal range—6 pA to 10 μAA from a multiplexed array of working electrodes to support a diversity of biosensor interfaces. A prototype microsystem was constructed by using the amperometric readout chip and an electrode array modified with secondary alcohol dehydrogenase enzyme. Test results demonstrate the proper operation of the circuit and the overall system; high linearity $(\mathrm{R}^2 = 0.998)$ between the measured biosensor responses and the target analyte (2-propanol) concentrations was observed. This system overcomes many challenges in interfacing biological recognition elements and microelectronic components to construct a miniaturized electrochemical protein-based biosensor array.

Acknowledgment

The authors would like to thank the MOSIS service for their support of during the development of the amperometric electrochemical readout circuit. They would also like to thank Dr. J. G. Zeikus for providing the enzyme used.

References

[1] M. I. Prodromidis and M. I. Karayannis, "Enzyme based amperometric biosensors for food analysis," *Electroanalysis*, vol. 14, pp. 241–261, Mar. 2002.

[2] B. L. Hassler and R. M. Worden, "Versatile bioelectronic interfaces based on heterotrifunctional linking molecules," *Biosensors Bioelectron.*, vol. 21, pp. 2146–2154, May 2006.

[3] M. U. Ahmed, M. M. Hossain, and E. Tamiya, "Electrochemical biosensors for medical and food applications," *Electroanalysis*, vol. 20, pp. 616–626, Mar. 2008.

[4] D. Grieshaber, R. MacKenzie, J. Voros, and E. Reimhult, "Electrochemical biosensors—Sensor principles and architectures," *Sensors*, vol. 8, pp. 1400–1458, Mar. 2008.

[5] S. F. Peteu, D. Emerson, and R. M. Worden, "A Clark-type oxidase enzyme-based amperometric microbiosensor for sensing glucose, galactose, or choline," *Biosensors Bioelectron.*, vol. 11, pp. 1059–1071, Nov. 1996.

[6] S. F. Peteu, M. T. Widman, and R. M. Worden, "In situ mapping of community-level cellular response with catalytic microbiosensors," *Biosensors Bioelectron.*, vol. 13, pp. 1197–1203, Nov. 1998.

[7] N. Kohli, D. Srivastava, J. Sun, R. J. Richardson, I. S. Lee, and R. M. Worden, "Nanostructured biosensor for measuring neuropathy target esterase activity," *Anal. Chemistry*, vol. 79, pp. 5196–5203, Jul. 2007.

[8] F. Laiwalla, K. G. Klemic, F. J. Sigworth, and E. Culurciello, "An integrated patch-clamp amplifier in silicon-on-sapphire CMOS," *IEEE Trans. Circuits Syst. I*, vol. 53, no. 11, pp. 2364–2370, Nov. 2006.

[9] M. Roham and P. Mohseni, "Wireless amperometric neurochemical monitoring using an integrated FSK telemetry circuit," in *Proc. 3rd Int. IEEE/EMBS Conf. Neural Engineering*, Kohala Coast, HI, 2007, pp. 159–162.

[10] R. J. Lipshutz, S. P. Fodor, T. R. Gingeras, and D. J. Lockhart, "High density synthetic oligonucleotide arrays," *Nature Genet. Suppl.*, vol. 21, pp. 24–29, Jan. 1999.

[11] M. Schena, D. Shalon, R. Heller, A. Chai, P. O. Brown, and R. W. Davis, "Parallel human genome analysis: Microarray-based expression monitoring of 1000 genes," *Proc. Nat. Acad. Sci.*, vol. 93, pp. 10614–10619, Oct. 1996.

[12] M. E. Bosch, A. J. R. Sanchez, F. S. Rojas, and C. B. Ojeda, "Optical chemical biosensors for high throughput screening of drugs," *Combinatorial Chem. High Throughput Screening*, vol. 10, pp. 413–432, Jul. 2007.

[13] M. Schena, *Microarray Analysis*. New York: Wiley, 2003.

[14] R. M. Worden, B. Hassler, P. Kim, N. Kohli, A. Mason, J. G. Zeikus, M. Laivenieks, and R. Ofoli, "Biomimetic interfaces for a multifunctional biosensor array microsystem," in *Proc. IEEE Int. Conf. Sensors*, Vienna, Austria, 2004, pp. 991–994.

[15] S. R. Jadhav, D. Sui, R. M. Garavito, and R. M. Worden, "Fabrication of highly insulating tethered bilayer lipid membrane using yeast cell membrane fractions for measuring ion channel activity," *J. Colloid Interface Sci.*, 2008, to be published.

[16] J. Prashar, P. Sharp, M. Scarffe, and B. Cornell, "Making lipid membranes even tougher," *J. Mater. Res.*, vol. 22, pp. 2189–2194, Aug. 2007.

[17] M. Schienle, C. Paulus, A. Frey, F. Hofmann, B. Holzapfl, and P. Schindler-Bauer *et al.*, "A fully electronic DNA sensor with 128 positions and in-pixel A/D conversion," *IEEE J. Solid-State Circuits*, vol. 39, no. 12, pp. 2438–2445, Dec. 2004.

[18] X. Zhu and C. H. Ahn, "On-chip electrochemical analysis system using nanoelectrodes and bioelectronic CMOS chip," *IEEE J. Sensors*, vol. 6, no. 5, pp. 1280–1286, Oct. 2006.

[19] S. B. Prakash, M. Urdaneta, M. Christophersen, E. Smela, and P. Abshire, "In situ electrochemical control of electroactive polymer films on a CMOS chip," *Sensors Actuators B: Chem.*, vol. 129, pp. 699–704, Feb. 2008.

[20] M. Breten, T. Lehmann, and E. Braun, "Integrating data converters for picoampere currents from electrochemical transducers," in *Proc. IEEE Int. Symp. Circuits and Systems*, San Francisco, CA, 2000, pp. 709–712.

[21] R. Genov, M. Stanacevic, M. Naware, G. Cauwenberghs, and N. Thakor, "16-channel integrated potentiostat for distributed neurochemical sensing," *IEEE Trans. Circuits Syst. I*, vol. 53, no. 11, pp. 2371–2376, Nov. 2006.

[22] A. Gore, S. Chakrabartty, S. Pal, and E. C. Alocilja, "A multichannel femtoampere-sensitivity potentiostat array for biosensing applications," *IEEE Trans. Circuits Syst. I*, vol. 53, no. 11, pp. 2357–2363, Nov. 2006.

[23] R. G. Kakerow, H. Kappert, E. Spiegel, and Y. Manoli, "Low-power single-chip CMOS potentiostat," in *Proc. Int. Conf. Solid-State Sensors and Actuators (Transducers)*, 1995, pp. 142–145.

[24] H. S. Narula and J. G. Harris, "VLSI potentiostat for amperometric measurements for electrolytic reactions," in *Proc. IEEE Int. Symp. Circuits Syst.*, Vancouver, BC, Canada, 2004, pp. 457–460.

[25] M. Stanacevic, K. Murari, A. Rege, G. Cauwenberghs, and N. V. Thakor, "VLIS potentiostat array with oversampling gain modulation for wide-range neurothransmitter sensing," *IEEE Trans. Biomed. Circuits Syst.*, vol. 1, no. 1, pp. 63–72, Jan. 2007.

[26] R. F. B. Turner, D. J. Harrison, and H. P. Baltes, "A CMOS potentiostat for amperometric chemical sensors," *IEEE J. Solid-State Circuits*, vol. 22, no. 3, pp. 473–478, Jun. 1987.

[27] M. Zayats, E. Katz, and I. Willner, "Electrical contacting of flavoenzymes and NAD(P)(+)-dependent enzymes by reconstitution and affinity interactions on phenylboronic acid monolayers associated with Au-electrodes," *J. Amer. Chem. Soc.*, vol. 124, pp. 14724–14735, Dec. 11, 2002.

[28] J. Zhang, Y. Huang, N. Trombly, C. Yang, and A. Mason, "Electrochemical array microsystem with integrated potentiostat," in *Proc. IEEE Int. Sensors Conf.*, Irving, CA, 2005, pp. 385–388.

[29] Y. Huang and A. Mason, "Post CMOS compatible microfabrication of a multi-analyte bioelectrochemcial sensor array microsystem," in *Proc. IEEE Int. Conf. Sensors*, Dageu, Korea, 2006, pp. 612–615.

[30] C. C. Enz and G. C. Temes, "Circuit techniques for reducing the effects of op-amp imperfections: Autozeroing, correlated double sampling, and chopper stabilization," *Proc. IEEE*, vol. 84, no. 11, pp. 1584–1614, Nov. 1996.
[31] J. Zhang, N. Trombly, and A. Mason, "A low noise readout circuit for integrated electrochemical biosensor arrays," in *Proc. IEEE Int. Conf. Sensors*, Vienna, Austria, 2004, pp. 36–39.
[32] P. R. Gray, P. J. Hurst, S. H. Lewis, and R. G. Meyer, *Analysis and Design of Analog Integrated Circuits*. New York: Wiley, 2001.
[33] Y. Wang, H. Xu, J. M. Zhang, and G. L. , *Sensors*, vol. 8, no. 4, pp. 2043–2081, 2008.
[34] N. Nikolaus and B. Strehlitz, "Amperometric lactate biosensors and their application in (sports) medicine, for life quality and wellbeing," *Microchimica Acta*, vol. 160, no. 1–2, pp. 15–55, 2008.
[35] B. L. Hassler, M. Dennis, M. Laivenieks, J. G. Zeikus, and R. M. Worden, "Mutation of Tyr-218 to Phe in thermoanaerobacter ethanolicus secondary alcohol dehydrogenase: Effects on bioelectronic interface performance," *Appl. Biochem. Biotechnol.*, vol. 143, pp. 1–15, Oct. 2007.

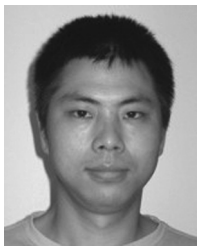

Chao Yang received the B.S. and M.S. degrees in electrical engineering from Tsinghua University, Beijing, China, in 1999 and 2002, respectively, and the Ph.D. degree in electrical engineering from Michigan State University, East Lansing, in 2008.

His research focus is the analog/mixed-signal integrated-circuit design for the biomedical and biochemical instrumentation microsystem. Currently, he is with Marvell Semiconductor, Inc., Santa Clara, CA.

Dr. Yang was the recipient of the Excellence Scholarships from Tsinghua University from 1996 to 1998 and the VLSI/SOC Fellowship from Michigan State University in 2007. He won third (out of 40) place in the phase-1 and phase-2 Semiconductor Research Corporation)/Semiconductor Industry Association SoC Design Challenge.

Yue Huang (S'07) received the B.S. degree in transportation engineering from Southwest Jiaotong University, Chengdu, China, in 1996, the M.S. degree in electrical engineering from Michigan State University, East Lansing, in 2007, where he is currently pursuing the Ph.D. degree in electrical engineering.

His research covers several aspects of enzyme-based integrated biosensors, including digital/analog integrated circuits, biochemistry, electrochemistry, microfabrication, microfluidics, and microelectromechanical systems.

Mr. Huang is a member of the Project Management Institute.

Brian L. Hassler received the B.S. (Hons.) degree in chemical engineering from Michigan Technological University, Houghton, in 2002 and is currently pursuing the Ph.D. degree at Michigan State University, East Lansing.

His research addresses the fabrication of bioelectronic interfaces using cofactor-dependent dehydrogenase enzymes. He has developed several bioelectronic interfaces suitable for applications in biosensors and biocatalysis as well as a mathematical model that describes the performance properties of the interfaces.

Mr. Hassler is a member of the American Chemical Society, the American Institute of Chemical Engineers, and the Electrochemical Society.

R. Mark Worden received the B.A. degree with a double major in chemistry and cell biology, the M.S. degree in chemical engineering, and the Ph.D. degree in chemical engineering from the University of Tennessee, Knoxville, in 1979, 1982, and 1986, respectively.

The research for the M.S. and Ph.D. degrees was conducted in the Bioprocess Engineering Group at Oak Ridge National Laboratory, Oak Ridge, TN. He became an Assistant Professor in the Department of Chemical Engineering and Materials Science at Michigan State University, East Lansing, in 1986, was promoted to Associate Professor in 1991, and then Professor in 1998. His research program integrates recombinant-protein production, biocatalysis, and nanotechnology to develop new systems for bioproduction, biosensing, and bioremediation. His current projects include the use of electrochemical sensor arrays for high-throughput biosensor systems and functional proteomics.

Andrew J. Mason (S'90–M'99–SM'06) received the B.S. degree in physics (Hons.) from Western Kentucky University, Bowling Green, in 1991, the B.S.E.E. degree (Hons.) from the Georgia Institute of Technology, Atlanta, in 1992, and the M.S. and Ph.D. degrees in electrical engineering from The University of Michigan, Ann Arbor, in 1994 and 2000, respectively.

From 1999 to 2001, he was an Assistant Professor at the University of Kentucky, Lexington. In 2001, he joined the Department of Electrical and Computer Engineering at Michigan State University, East Lansing, where he is currently an Associate Professor. His research addresses many areas of mixed-signal circuit design and the fabrication of integrated microsystems. Current projects include compact low-power bioelectrochemical interrogation circuits, adaptive chemical sensor interface circuits, post-complementary metal–oxide semiconductor fabrication of electrochemical sensor arrays, and mixed-signal integrated circuits for signal processing in neural implants.

Dr. Mason serves on the Sensory Systems and Biomedical Circuits and Systems Technical Committees of the IEEE Circuits and Systems Society and on the Technical Program Committee of the IEEE International Conference on Sensors. He received the Michigan State University Teacher-Scholar Award in 2006.